

Report: Application of Projection Method and Staggered Grid to Incompressible Navier-Stokes Equations

Mohamed Mohsen Ahmed
Kansas State University, Manhattan, Kansas, USA

This article presents a finite difference numerical method based on projection method for solving 2-D incompressible Navier-Stokes equation. Numerical implementation of the method in a FORTRAN solver is presented. Simulations are performed on a 2-D lid driven cavity at different Reynolds number and comparisons are conducted with benchmark solutions found in the literature in order to verify the solver and provide confidence that the solver is free from any coding errors.

I. Nomenclature

k	=	iteration number
M	=	number of mesh points in x direction
N	=	number of mesh points in y direction
n	=	n-th time step
p	=	normalized pressure
Re	=	Reynolds number
t	=	time
u	=	normalized velocity component in x direction
v	=	normalized velocity component in y direction

II. Introduction

Navier-Stokes equations are derived from rational continuum mechanics to generally describe the behavior of Newtonian fluids at different conditions. These equations are non-linear second order coupled partial differential equations that an exact solution can only be obtained if certain approximations are performed. Therefore, numerical solutions of Navier-Stokes equations are the most practical method for engineering application involving complex flows.

We are concerned here with the numerical solution of the 2-Dimensional incompressible Navier-Stokes equations. The governing equations in the non-dimensionalized primitive variable form are

1) continuity equation

$$\frac{\partial u}{\partial x} + \frac{\partial v}{\partial y} = 0 \quad (1)$$

2) Momentum equation x-direction

$$\frac{\partial u}{\partial t} + \frac{\partial u^2}{\partial x} + \frac{\partial uv}{\partial y} + \frac{\partial p}{\partial x} = \frac{1}{Re} \left(\frac{\partial^2 u}{\partial x^2} + \frac{\partial^2 u}{\partial y^2} \right) \quad (2)$$

3) Momentum equation y-direction

$$\frac{\partial v}{\partial t} + \frac{\partial uv}{\partial x} + \frac{\partial v^2}{\partial y} + \frac{\partial p}{\partial y} = \frac{1}{Re} \left(\frac{\partial^2 v}{\partial x^2} + \frac{\partial^2 v}{\partial y^2} \right) \quad (3)$$

Finite difference method is employed to discretize the governing equations on a staggered grid. The use of staggered grid allows the coupling between u , v and p at adjacent point, thus, preventing oscillations and checker-board effects. The classical description of staggered grid is shown in Figure 1. In the classical description, the pressure is located at cell center points i, j . It can be discretized using second order central scheme about point $i + 1/2, j$ such that

$$\frac{\partial p}{\partial x} = \frac{p_{i+1,j} - p_{i,j}}{\Delta x} \quad (4)$$

and

$$\frac{\partial p}{\partial y} = \frac{p_{i,j+1} - p_{i,j}}{\Delta y} \quad (5)$$

In the classical description of staggered grid, the x component of the velocity u is defined at points $i + 1/2, j$, while the y component of the velocity v is defined at points $i, j + 1/2$. An alternative notation is introduced since the classical description of the points corresponding to velocity components u and v , i.e. $i + 1/2, j$ and $i, j + 1/2$, can not be employed in programming languages loops. As shown in figure 2, the pressure is still defined at the cell center point i, j . However, the velocity components u and v can now be defined using the same indices of the pressure i, j but with careful consideration. The velocity components now are defined as u_f, u_b, v_f and v_b which correspond to forward and backward edges of the cell corresponding to point i, j . The velocity at the cell center point i, j can now be calculated from the average of the forward and backward velocities such that

$$u(i, j) = \frac{u_f(i, j) + u_b(i, j)}{\Delta x} \quad (6)$$

$$v(i, j) = \frac{v_f(i, j) + v_b(i, j)}{\Delta y} \quad (7)$$

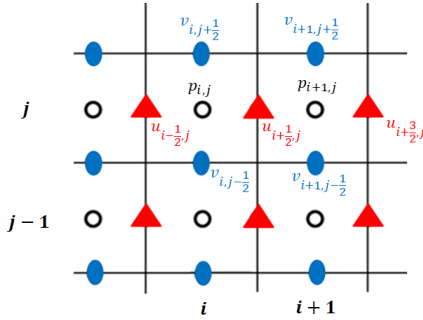


Fig. 1 Staggered Grid (classical description)

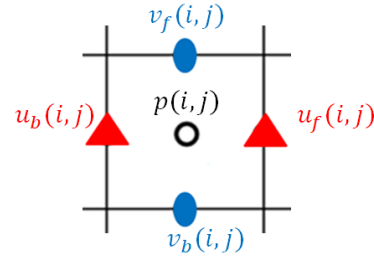


Fig. 2 Staggered Grid (current notation)

III. Marker and Cell (MAC) Method

Marker and Cell method (MAC) is a classical method introduced in 1965 for solving incompressible Navier-Stokes equations. The staggered grid described earlier is employed in the MAC method to solve the Pressure Poisson equation at every time step [1].

In current notation of staggered grid, the continuity equation can be discretized using central differencing about point i, j as

$$\frac{u_f(i, j) - u_b(i, j)}{\Delta x} + \frac{v_f(i, j) - v_b(i, j)}{\Delta y} \quad (8)$$

Explicit discretization of the x-momentum equation about point i, j using central differences yields

$$u_f^{n+1}(i, j) = F_f^n(i, j) - \frac{\Delta t}{\Delta x} [p(i+1, j) - p(i, j)]^{n+1} \quad (9)$$

where

$$\begin{aligned} F_f^n(i, j) = & u_f^n(i, j) + \Delta t \left[\frac{u_f(i+1, j) - 2u_f(i, j) + u_b(i, j)}{Re\Delta x^2} \right. \\ & + \frac{u_f(i, j-1) - 2u_f(i, j) + u_f(i, j+1)}{Re\Delta y^2} \\ & \left. - \frac{u^2(i+1, j) - u^2(i, j)}{\Delta x} - \frac{[uv]_{ff}(i, j) - [uv]_{fb}(i, j)}{\Delta y} \right]^n \end{aligned} \quad (10)$$

Similarly, the y-momentum equation is discretized as

$$v_f^{n+1}(i, j) = G_f^n(i, j) - \frac{\Delta t}{\Delta x} [p(i, j+1) - p(i, j)]^{n+1} \quad (11)$$

where

$$\begin{aligned} G_f^n(i, j) = & v_f^n(i, j) + \Delta t \left[\frac{v_f(i+1, j) - 2v_f(i, j) + v_f(i-1, j)}{Re\Delta x^2} \right. \\ & + \frac{u_f(i, j+1) - 2v_f(i, j) + v_b(i, j)}{Re\Delta y^2} \\ & \left. - \frac{v^2(i, j+1) - v^2(i, j)}{\Delta y} - \frac{[uv]_{ff}(i, j) - [uv]_{bf}(i, j)}{\Delta x} \right]^n \end{aligned} \quad (12)$$

The subscripts *ff*, *fb* and *bf* correspond to the corner points of the cell whose center is point *i, j*. The corresponding terms are

$$\begin{aligned} [uv]_{ff}(i, j) &= \left(\frac{u_f(i, j) - u_f(i, j+1)}{2} \right) \left(\frac{v_f(i, j) + v_f(i+1, j)}{2} \right) \\ [uv]_{fb}(i, j) &= \left(\frac{u_f(i, j) - u_f(i, j-1)}{2} \right) \left(\frac{v_f(i, j-1) + v_f(i+1, j-1)}{2} \right) \\ [uv]_{bf}(i, j) &= \left(\frac{u_f(i-1, j) - u_f(i-1, j+1)}{2} \right) \left(\frac{v_f(i, j) + v_f(i-1, j)}{2} \right) \end{aligned} \quad (13)$$

In order to close the system of equations, an additional pressure equation is introduced in MAC method. The pressure Poisson equation is obtained by substituting equations (9,11) into (8) such that

$$\left[\frac{p(i-1, j) - 2p(i, j) + p(i+1, j)}{\Delta x^2} + \frac{p(i, j-1) - 2p(i, j) + p(i, j+1)}{\Delta y^2} \right]^{n+1} = R^n(i, j) \quad (14)$$

where

$$R^n(i, j) = \frac{1}{\Delta t} \left[\frac{F_f(i, j) - F_b(i, j)}{\Delta x} + \frac{G_f(i, j) - G_b(i, j)}{\Delta y} \right]^n \quad (15)$$

Since MAC algorithm provides an explicit expression of the momentum equation, limitations are introduced on the maximum time step for a stable solution. Peyret and Taylor [2] provided a correlation between the time step, Reynolds number and mesh size. If $\Delta x = \Delta y$ the restriction is

$$\frac{\Delta t}{Re \Delta x^2} \leq 0.25 \quad (16)$$

MAC method requires a boundary conditions to be specified for each *u, v* and *p*. No slip boundary condition is the physical boundary condition defined for the velocity while the pressure gradient is assumed to vanish near the walls. Details on the numerical implementation of the boundary conditions is provided in the next section.

IV. Solver Algorithm

Now we have all equations in a discretized form, the next step is to implement these equations in a FORTRAN code. Since the pressure equation is implicit, i.e. requires all mesh points to be solved simultaneously, it requires a matrix solver. Alternative Direct Implicit method (ADI) is employed to solve the pressure Poisson equation. In this method, the solution of each grouped row is obtained using Thomas Algorithm of tri-diagonal matrices. Then, the process is repeated for each grouped column to complete one iteration cycle of ADI method. The iteration cycle is repeated until the infinity norm of the pressure reaches a convergence criteria of 10^{-9} . The overall FORTRAN solver algorithm is explained in the flowchart of figure 3.

V. Results and Discussion

A square cavity of unity length, shown in figure 4, is considered for validation and verification purposes. The top wall is moving with speed $v_w = 1$ and all other walls are not moving. Different grid sizes are considered for each

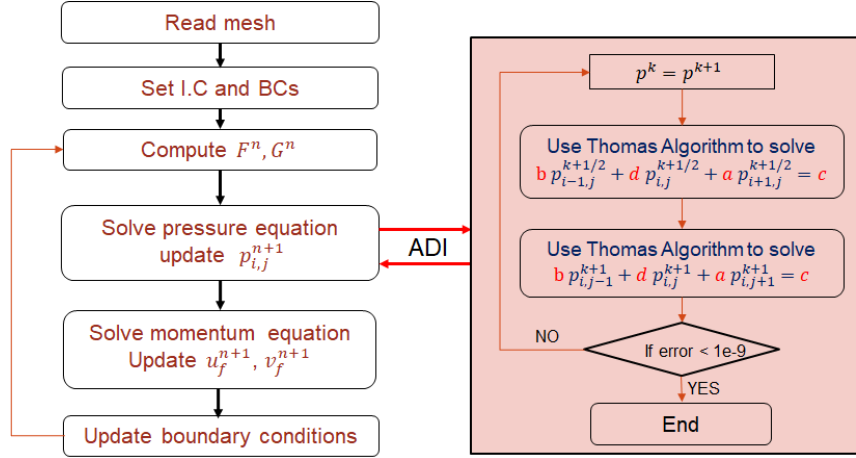


Fig. 3 Solver algorithm

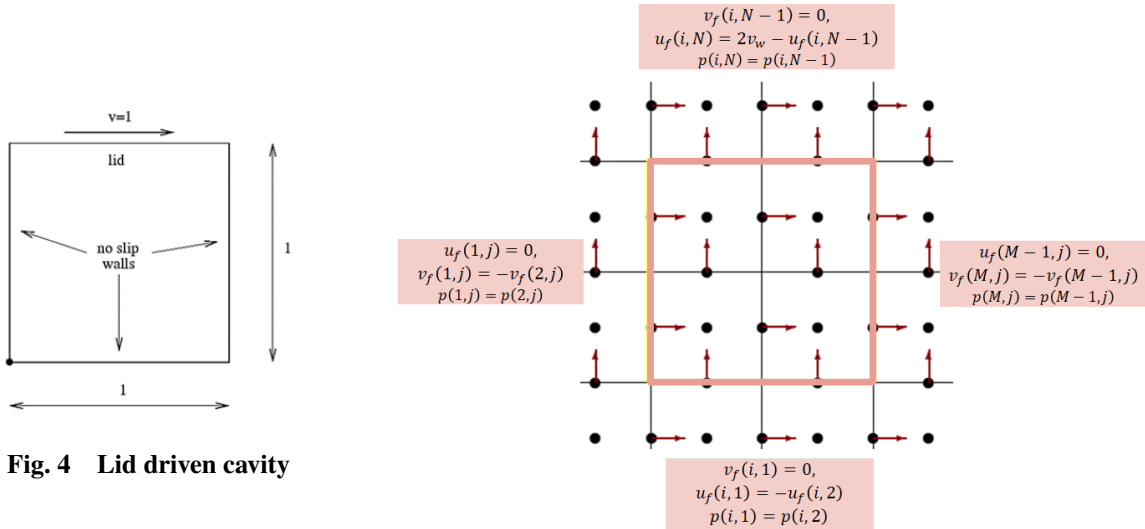


Fig. 4 Lid driven cavity

Fig. 5 Boundary conditions

simulated case. Ghost cells are introduced on the staggered grid to specify the constraints of the boundary points. No slip and zero pressure gradient are specified on all walls. The numerical implementation of the boundary conditions is specified in figure 5.

A study on the mesh size effect on the solution is performed first at a Reynolds number of 100. Then, different the finest mesh is used to simulate different Reynolds number cases.

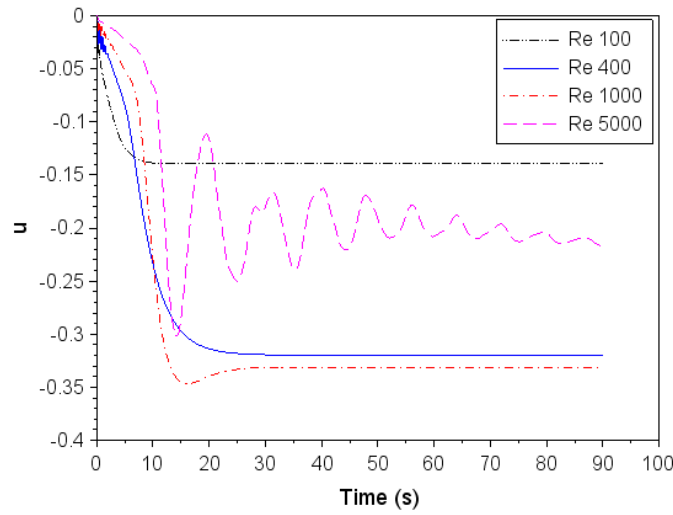
As mentioned earlier, the stability of the problem is very sensitive to the choice of the time step. Thus, the correlation obtained from equation 16 is employed and extended to different Reynolds number cases. It is found that the correlation needs have more restriction for high Reynolds number cases. A summary of the simulated cases including the Reynolds number and the time step is listed in table 1.

In order to monitor the transient behavior and decide whether or not the solution reached steady state, an arbitrary point inside the computational domain is chosen and the velocity is plotted at each time step. The monitoring point location is (0.5, 0.25). As shown in figure 6, the transient behavior of Reynolds number up to 1000 is smooth and the solution reaches steady state much earlier compared to Reynolds 5000 in which the solutions has some oscillations.

Further analysis are carried out on the steady state solution of each case. A qualitative comparison is carried out between the current solution and two different benchmark solutions by Ghia et al. [3] and Kim and Moin [4]. Figure 7 shows the distribution of u velocity along y -direction at $x = 0.5$ for different mesh levels at $Re = 100$ when the solution reached steady state (time=17.24 s). It can be inferred that a grid independent solution can be obtained at mesh level

Table 1 Summary of simulated cases

Reynolds Number	Mesh size	Time step (s)	Restriction
100	20x20	0.07407	$\Delta t = 0.24Re(\Delta x)^2$
	40x40	0.01662	
	60x60	7.134e-3	
	120x120	1.724e-3	
400	120x120	6.895e-3	$\Delta t = 0.24Re(\Delta x)^2$
1000	120x120	7.182e-3	$\Delta t = 0.1Re(\Delta x)^2$
5000	120x120	8.977e-4	$\Delta t = 0.0025Re(\Delta x)^2$

**Fig. 6 Instantaneous u velocity at monitoring location (0.5, 0.25)**

60x60 or above. Also, the solution is in good agreement with the benchmark solution of Ghia et al. Furthermore, a qualitative comparison of the vorticity between current and benchmark solution, shown in figure 8, show that the current solver accurately predicts the vorticity contours. Additional contours of pressure, velocity components and streamlines are shown in figure 9. It can be inferred that there exist a single main vortex which center is shifted near the top right corner of the cavity. Also, the pressure is uniform except near the top left corner where an expansion exist and near the top right corner where a compression exist due to the vortex motion against the wall.

Similar comparison is carried out for the case of $Re = 400$ at time = 41.37 s. Figures 10 and 11 provide both quantitative and qualitative comparisons between the current solution and the benchmark solution of Ghia et al. and Kim and Moin. Both comparisons reveal good agreement in terms of velocity distribution and vorticity contours. It is observed that the main vortex is shifted closer to the right top wall and a small vortex is created near the bottom right corner.

The distributions of u velocity for high Reynolds number cases $Re = 1000$ and $Re = 5000$ are plotted in figures 12 and 13 respectively and compared with the benchmark solution of Ghia et al. Good agreement is obtained which confirms that the solver is able to accurately predict the flow behavior at high Reynolds number and provides a stable solution. Additional qualitative comparison is provided in figure 14 for the vorticity contours of both cases.

Contours of pressure, velocity and stream function are shown in figures 15 and 16 for the cases of $Re = 1000$ and $Re = 5000$ respectively. The main vortex now is moving back towards the center of the cavity. Moreover, two secondary vortices are created near the bottom left and bottom right corners.

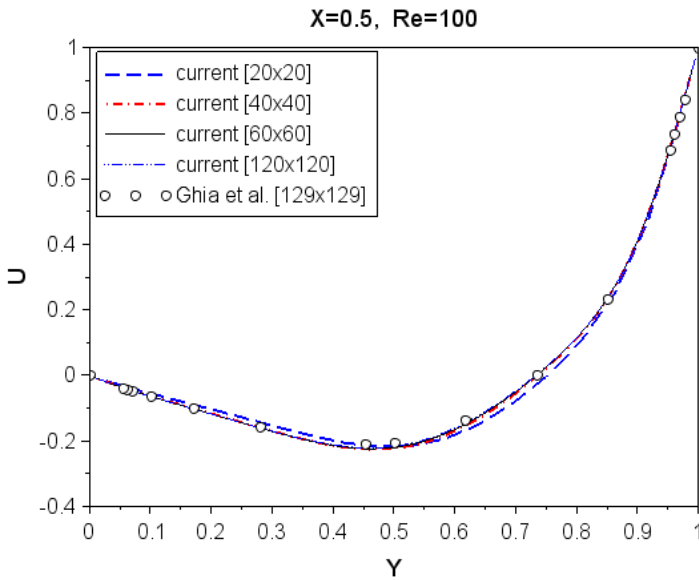


Fig. 7 distribution of u at $x = 0.5$ for $Re = 100$

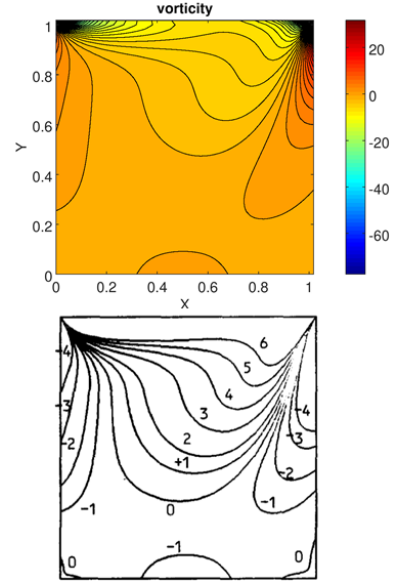


Fig. 8 $Re = 100$ Vorticity contours, top: current solution, bottom Ghia et al. [3]

VI. Conclusion

Marker and Cell method is applied to Incompressible Navier-Stokes equations on a staggered grid. The new notation describing the velocities at the cell edge provide a simple way of treating all variables with same array counters, thus making programming much simpler. A finite difference FORTRAN code is developed and applied to the problem of lid driven cavity. Five Reynolds number cases are simulated. It is found that the time step has to be adjusted for each Reynolds number. New correlation is provided which gives more restriction at high Reynolds number compared to that provided by Peyret and Taylor [2]. Comparison between current simulations and benchmark simulations of Ghia et al. [3] and Kim and Moin [4] reveal good agreement and provides us with confidence that the solver is validated and free from any coding errors.

VII. Acknowledgment

The author would like to thank Dr. Mingjun Wei for his guidance and contribution to this work.

References

- [1] Fletcher, C. A., *Computational techniques for fluid dynamics 2: Specific techniques for different flow categories*, Springer Science & Business Media, 2012.
- [2] Peyret, R., and Taylor, T. D., *Computational methods for fluid flow*, Vol. 11, Springer-Verlag, New York, 1983.
- [3] Ghia, U., Ghia, K. N., and Shin, C., "High-Re solutions for incompressible flow using the Navier-Stokes equations and a multigrid method," *Journal of computational physics*, Vol. 48, No. 3, 1982, pp. 387–411.
- [4] Kim, J., and Moin, P., "Application of a fractional-step method to incompressible Navier-Stokes equations," *Journal of computational physics*, Vol. 59, No. 2, 1985, pp. 308–323.

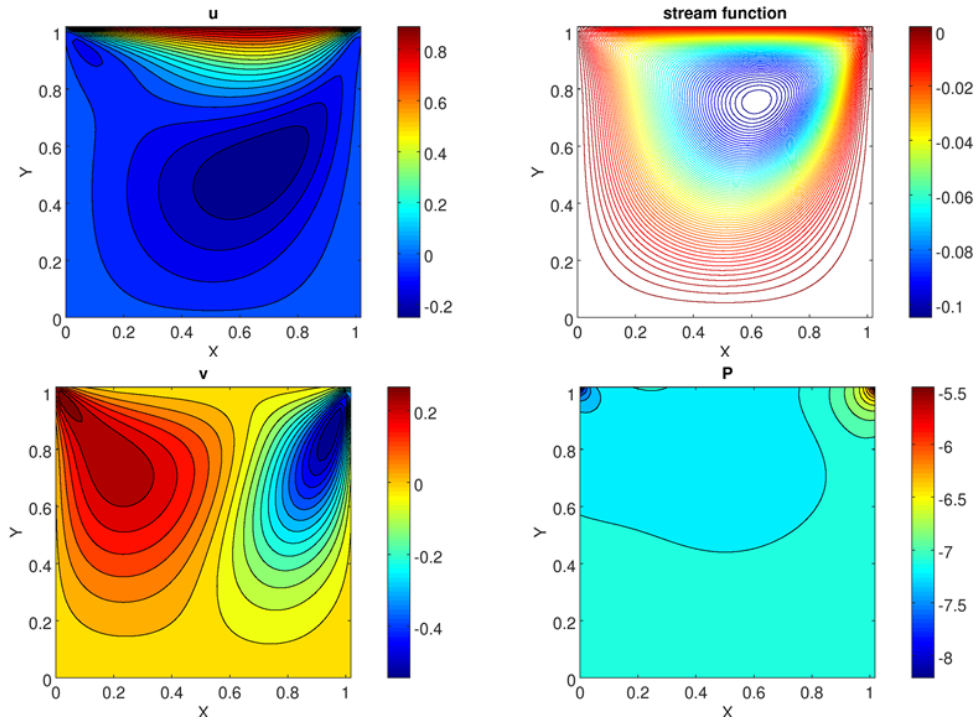


Fig. 9 $Re = 100$ Contours of pressure, velocity and stream function

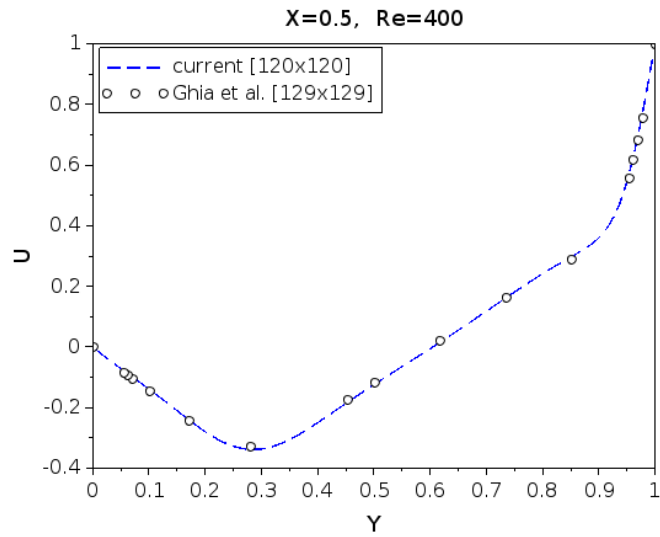


Fig. 10 distribution of u at $x = 0.5$ for $Re = 400$

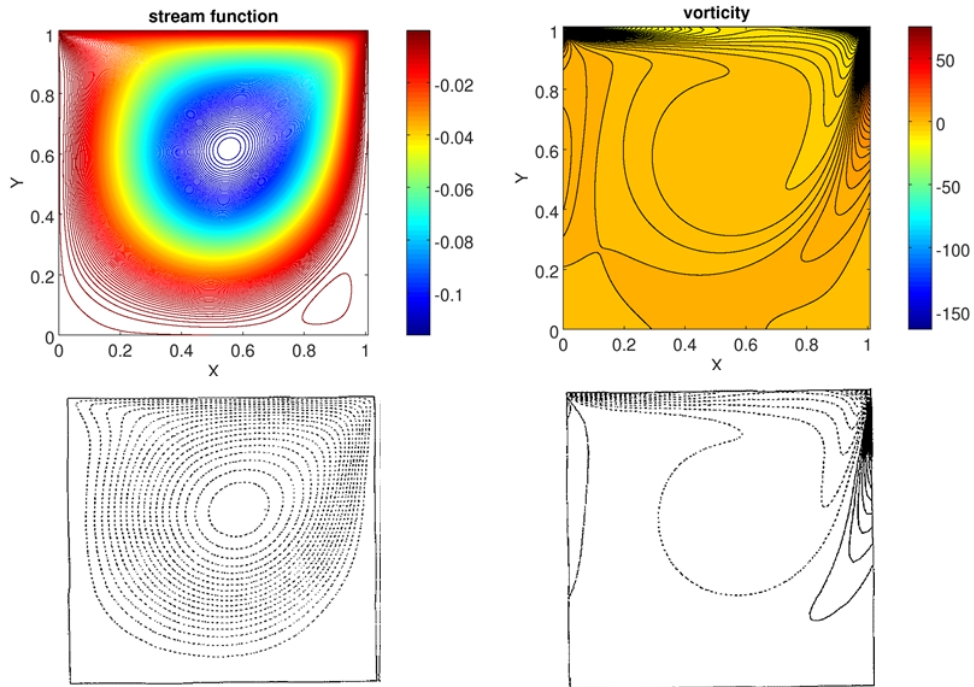


Fig. 11 Re 400 Vorticity and stream function contours, top: current solution, bottom Kim and Moin. [4]

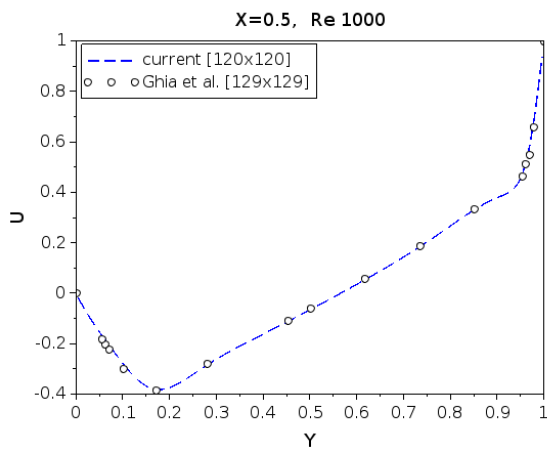


Fig. 12 Distribution of u at $x = 0.5$ for $Re = 1000$

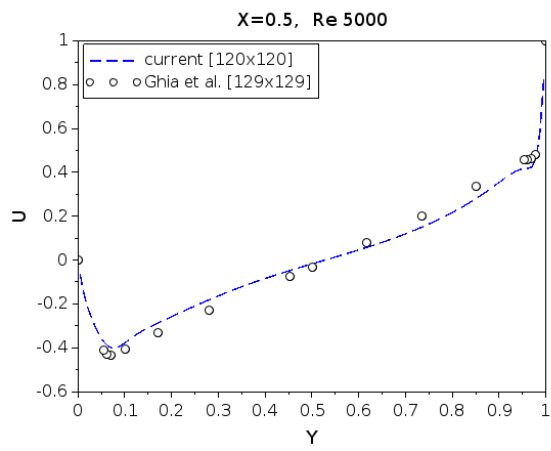


Fig. 13 Distribution of u at $x = 0.5$ for $Re = 5000$

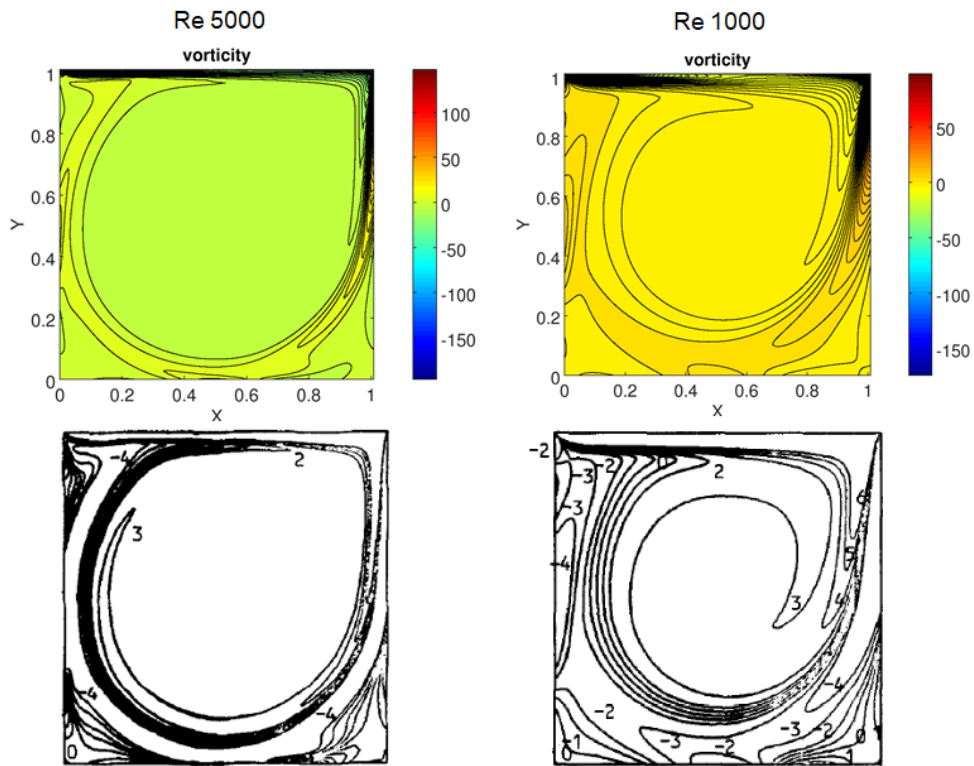


Fig. 14 Vorticity contours, top: current solution, bottom Ghia et al. [3]

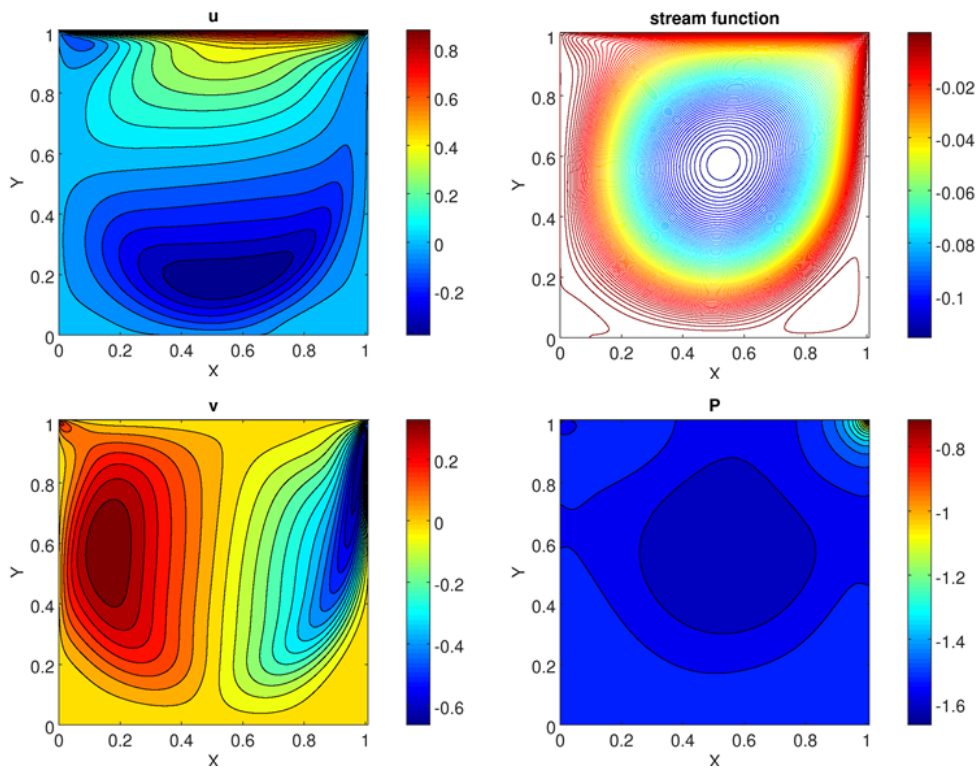


Fig. 15 Re 1000 Contours of pressure, velocity and stream function

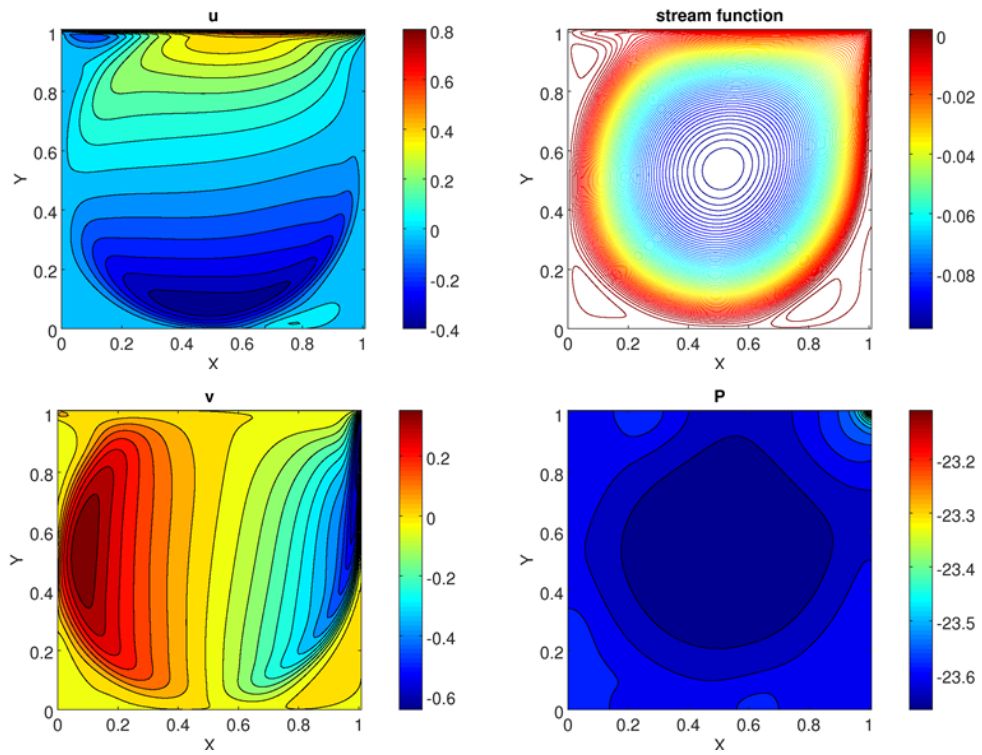


Fig. 16 Re 5000 Contours of pressure, velocity and stream function